Title

Opioidergic signaling contributes to food-mediated suppression of AgRP neurons.

Journal

Cell Reports, 43(1)

Authors

Sayar-Atasoy, Nilufer

Yavuz, Yavuz

Laule, Connor

et al.

Publication Date

2024-01-23

DOI

10.1016/j.celrep.2023.113630

Peer reviewed

HHS Public Access

Author manuscript

Cell Rep. Author manuscript; available in PMC 2024 February 14.

Published in final edited form as:

Cell Rep. 2024 January 23; 43(1): 113630. doi:10.1016/j.celrep.2023.113630.

Opioidergic signaling contributes to food-mediated suppression of AgRP neurons

Nilufer Sayar-Atasoy[1,6], **Yavuz Yavuz**[1,2,6], **Connor Laule**[1], **Chunyang Dong**[3], **Hyojin Kim**[1], **Jacob Rysted**[1], **Kyle Flippo**[1], **Debbie Davis**[1], **Iltan Aklan**[1], **Bayram Yilmaz**[2], **Lin Tian**[3], **Deniz Atasoy**[1,4,5,7,*]

[1]Department of Neuroscience and Pharmacology, Roy J. and Lucille A. Carver College of Medicine, University of Iowa, Iowa City, IA 52242, USA

[2]Department of Physiology, School of Medicine, Yeditepe University, Istanbul 34755, Turkey

[3]Department of Biochemistry and Molecular Medicine, School of Medicine, University of California, Davis, Davis, CA 95616, USA

[4]Iowa Neuroscience Institute, Roy J. and Lucille A. Carver College of Medicine, University of Iowa, Iowa City, IA 52242, USA

[5]Fraternal Order of Eagles Diabetes Research Center (FOEDRC), Roy J. and Lucille A. Carver College of Medicine, University of Iowa, Iowa City, IA 52242, USA

[6]These authors contributed equally

[7]Lead contact

SUMMARY

Opioids are generally known to promote hedonic food consumption. Although much of the existing evidence is primarily based on studies of the mesolimbic pathway, endogenous opioids and their receptors are widely expressed in hypothalamic appetite circuits as well; however, their role in homeostatic feeding remains unclear. Using a fluorescent opioid sensor, deltaLight, here we report that mediobasal hypothalamic opioid levels increase by feeding, which directly and indirectly inhibits agouti-related protein (AgRP)-expressing neurons through the μ-opioid receptor (MOR). AgRP-specific MOR expression increases by energy surfeit and contributes to opioid-induced suppression of appetite. Conversely, its antagonists diminish suppression of AgRP neuron activity by food and satiety hormones. Mice with AgRP neuron-specific ablation of MOR

*Correspondence: deniz-atasoy@uiowa.edu.

AUTHOR CONTRIBUTIONS

N.S.-A. performed fiber photometry recording experiments, behavioral experiments, surgeries, and genotyping and prepared MATLAB codes for data acquisition and the figures. Y.Y., C.L., and I.A. performed electrophysiological recordings. B.Y. contributed to logistics and reagents. D.D. managed mouse handling. H.K., J.R., C.L., and N.S.-A. contributed to post hoc analysis. K.F. analyzed gene expression data. C.D. and L.T. developed and provided the fluorescent opioid sensor. D.A., N.S.-A., and Y.Y. conceived experiments, analyzed data, and wrote the manuscript.

SUPPLEMENTAL INFORMATION

Supplemental information can be found online at https://doi.org/10.1016/j.celrep.2023.113630.

DECLARATION OF INTERESTS

The authors declare no competing interests.

expression have increased fat preference without increased motivation. These results suggest that post-ingestion release of endogenous opioids contributes to AgRP neuron inhibition to shape food choice through MOR signaling.

Graphical Abstract

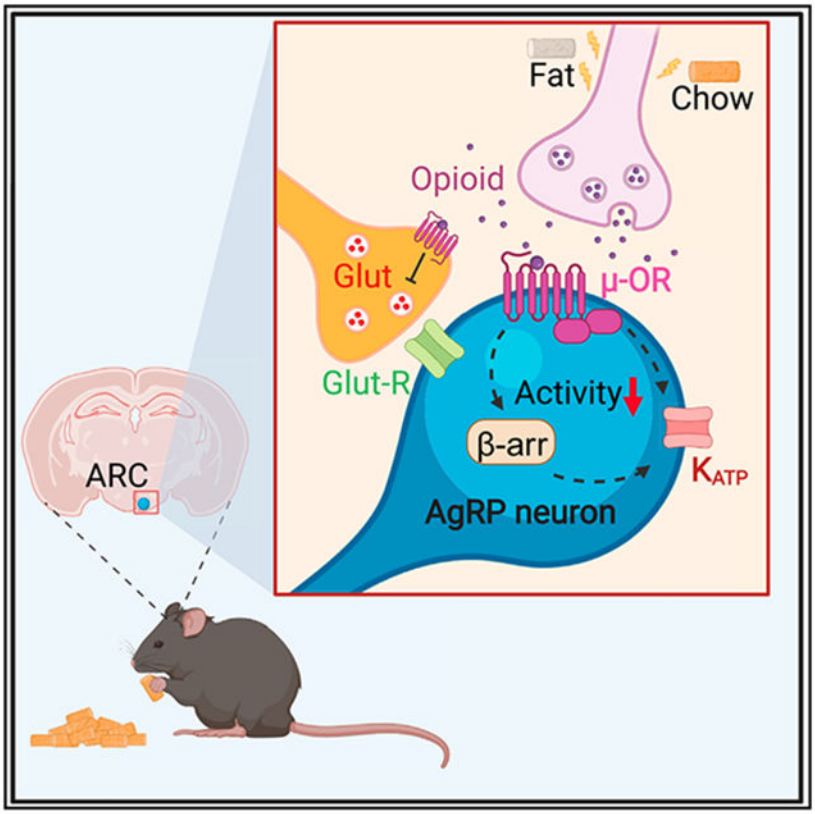

In brief

Sayar-Atasoy et al. show that feeding increases endogenous opioid levels in the hypothalamus, where they inhibit the hunger-promoting AgRP neurons to restrain further consumption.

INTRODUCTION

Progression and maintenance of obesity is associated with a number of sustained biochemical changes in brain transmitter levels. Both human imaging studies and biochemical measurements from animal models have established dysregulation of opioidergic signaling in obese subjects,[1,2] which can be restored by weight loss through diet or bariatric surgery.[3,4] On the other end, increased plasma and cerebrospinal fluid β-endorphin levels are associated with eating disorders.[5-8]

Opioids have a complex relationship with feeding behavior. Based on a large body of pharmacologic and genetic ablation studies that are primarily focused on reward pathways, it is generally thought that opioids facilitate hedonic appetite.[9,10] However, endogenous

opioid peptides and their receptors are also widely expressed throughout the hypothalamic regions that are involved in homeostatic appetite regulation. These neuron populations, such as pro-opiomelanocortin (POMC) and pro-dynorphin (PDYN), are activated by food intake, and their activation suppresses feeding.[11-13] Therefore, contrary to its established function, hypothalamic opioid signaling may not be orexigenic.

To better understand the role of hypothalamic opioid signaling in feeding, here we addressed its role in homeostatic hunger pathways. We found that consuming palatable and nonpalatable food increases hypothalamic opioid release, which can directly inhibit AgRP neurons to promote satiety.

RESULTS

Feeding increases opioid levels in the mediobasal hypothalamus

Previous work has shown that palatable food increases endogenous opioid release but provided limited temporal and anatomical resolution.[14] To better understand opioid dynamics in response to feeding, we used deltaLight, a genetically encoded opioid sensor based on the δ-opioid receptor (DOR).[15] We targeted the AAV-hSyn-deltaLight viral vector into the arcuate hypothalamic nucleus (ARC) to monitor *in vivo* opioid levels with fiber photometry (Figures 1A-1C). Presentation of chow food, but not inedible objects, to fasted mice slowly increased mediobasal opioid levels, as determined from the rise in photometry signal (Figures 1D and 1E), and this pattern was specific to the deltaLight sensor (Figures S1A-S1C). This increase was not observed in freely feeding mice (Figures S1D and S1E). Notably, the surge in opioid signaling during chow refeeding took more than 10 min to reach peak, and presentation of inaccessible food alone did not cause a significant shift in deltaLight signal, suggesting that sensory food detection is not sufficient, and ingestion was required (Figures S1F and S1G). Contrary to the lack of chow response in freely feeding mice, presentation of palatable food (high fat, high sugar [HFHS]) caused a robust increase in deltaLight signal (Figures 1F and 1G). Overall, these results show that feeding increases mediobasal hypothalamic opioid levels, suggesting that opioid release is not exclusive to the mesolimbic system or to palatable food. Moreover, hypothalamic opioid signaling was sensitive to both nutritional status and the palatability of food.

μ-Opioid receptor (MOR) agonism cell-autonomously suppresses AgRP neurons

Among the hypothalamic neuron populations that respond to feeding, rapid inhibition of AgRP neurons is well characterized.[11,16] Given the inhibitory nature of opioids, we next asked whether an endogenous opioid surge contributes to food-related AgRP neuron inhibition. We first tested whether AgRP neurons respond to opioids. For this, we performed *in vivo* fiber photometry imaging from GCaMP7s-expressing AgRP neurons using *Agrp-ires-cre* mice (Figure 2A). Because deltaLight has higher selectivity for enkephalin and β-endorphin, we focused on targeting their receptors, DOR and MOR, respectively. Systemic injection of SNC162, a selective DOR agonist, had no detectable effect on AgRP neuron activity, whereas DAMGO, a selective MOR agonist, rapidly suppressed it (Figures 2B, 2C, S2A, and S2B). The amount of DAMGO-induced suppression was comparable with that observed after chow presentation or a cocktail of satiety hormones (Figure S2E).

Because opioid receptors are widely expressed in hypothalamic circuits, their global activation may indirectly influence AgRP neurons. Thus, we next asked whether DAMGO acts directly on AgRP neurons. We prepared acute brain slices from *Npy-gfp* mice and performed electrophysiological recordings from GFP^+ NPY neurons in the ARC, which have been established to have near-complete overlap with AgRP neurons.[17] Consistent with *in vivo* activity imaging, loose seal recordings in the presence of synaptic blockers showed a drastic reduction in AgRP neuron activity upon bath application of DAMGO (Figures 2D-2F). Conversely, activation of DOR with SNC162 under the same conditions had no detectable impact (Figures S2C and S2D).

To further verify the cell-autonomous nature of MOR-dependent inhibition of AgRP neurons, in the presence of synaptic blockers, we blocked downstream G-protein signaling specifically in AgRP neurons by replacing intracellular GTP with GDPβS through the recording pipette, which competitively inhibits the G-protein cycle. Consistent with cell-autonomous inhibition, DAMGO caused rapid hyperpolarization of AgRP neurons, which was completely blocked with a high dose of intracellular GDPβS (2.4 mM), suggesting that G-protein activation is required within AgRP neurons (Figures 2G-2J).

Remarkably, a lower dose of intracellular GDPβS (0.8 mM) was ineffective at blocking DAMGO-mediated hyperpolarization (Figures S3A and S3B) with similar dialysis times (~10 min). However, addition of compound 101 (cmp101), an inhibitor of hypothalamus-enriched GRK2/3,[18] significantly reduced DAMGO-induced hyperpolarization under these conditions, whereas cmp101 alone had no effect (Figures S3C-S3F). This suggests that a branch of the MOR downstream pathway recruits β-arrestin and can only be unveiled under partial G-protein inhibition. Previously, a β-arrestin-phosphatidylinositol 3-kinase (PI3K)-K_{ATP} pathway has been shown to mediate insulin receptor (IR)-dependent hyperpolarization of AgRP neurons.[19,20] Therefore, we hypothesized that MOR-dependent activation of β-arrestin signaling and subsequent hyperpolarization, an effect unmasked with low intracellular GDPβS, may rely on a PI3K pathway. Consistently, pharmacological inhibition of PI3K by wortmannin completely blocked DAMGO-mediated hyperpolarization under conditions of low intracellular GDPβS (Figures S3G and S3H). Similarly, inhibition of the putative downstream K_{ATP} channel by tolbutamide abolished DAMGO-induced hyperpolarization (Figures S3I-S3K). Importantly, none of these inhibitors had a hyperpolarizing effect on their own that could have masked subsequent DAMGO-induced hyperpolarization. On the contrary, high internal GDPβS and wortmannin had a depolarizing influence (Figure S3L). Collectively, these experiments support the idea that both β-arrestin-dependent (MOR→GRK→β-arrestin→PI3K → K_{ATP}) and -independent pathways may contribute to MOR-mediated AgRP neuron hyperpolarization.

MOR activation can suppress network input and output of AgRP neurons

While our recordings establish the capacity of cell-autonomous opioid signaling to suppress AgRP neuron activity, this does not rule out a contribution of opioid signaling in the upstream network, which may indirectly suppress AgRP neurons. Consistently, in line with a previous report,[21] we found that DAMGO significantly suppressed the frequency of spontaneous excitatory postsynaptic currents (sEPSCs) recorded from AgRP neurons of

fasted mice (Figures 3A-3C), suggesting that MOR-based signaling can also potentially diminish AgRP neuron activity through its network actions.

Opioidergic signaling is well established to suppress output from synaptic terminals. We next tested whether this is also the case for AgRP neurons themselves. For this, we expressed Channelrhodopsin-2 (ChR2) specifically in AgRP neurons and recorded its synaptic output from PVN neurons, which we have shown previously to make a direct GABAergic connection.[22,23] In line with a previous report,[24] we found that synaptic GABA release from AgRP neurons onto downstream PVN neurons is significantly suppressed by DAMGO application in acute slice recordings (Figures 3D-3F), suggesting that opioidergic suppression of AgRP neuronal output can also occur distally, providing an additional level of inhibition.

Opioid signaling contributes to food-mediated suppression of AgRP neurons

Because both opioid release and AgRP neuron suppression are induced by feeding, we next asked whether these two are causally related; that is, whether opioidergic inhibition is responsible for food-induced suppression of AgRP neurons. Consistent with a role of opioid signaling in metabolic regulation, single-cell transcriptomics analysis from AgRP neurons showed increased MOR expression in fed mice compared with a fasted state (Figure S4A).[25] To test whether opioid signaling contributes to food-induced AgRP neuron inhibition, we performed *ex vivo* loose seal recordings from AgRP neurons of *ad libitum*-fed mice early in the morning, when they are expected to be sated. In agreement with opioid-mediated tonic suppression, naloxone perfusion significantly increased AgRP neuron activity (Figures 4A and 4B). This increase was metabolic state dependent because application of the MOR-specific antagonist CTAP to acute slices prepared from fasted mice did not cause a further increase in AgRP neuron activity (Figure S4B). Similarly, naloxone did not affect *in vivo* baseline AgRP neuron activity in fasted mice (Figures S4C and S4D).

These findings support a role of food-related opioidergic suppression of AgRP neurons *ex vivo.* To gain further insight *in vivo*, we performed Ca^{2+}-based fiber photometry imaging in fasted mice. As expected, AgRP neuron activity was rapidly suppressed with food access. We found that the amount of suppression was significantly reduced with intraperitoneal (i.p.) naloxone delivery (Figures 4C and 4D). However, we also noticed a significant reduction in food consumption (Figure S4E) which may contribute to reduced AgRP neuron suppression. Therefore, we repeated this measurement using a MOR-specific antagonist, CTAP, which did not reduce the chow refeeding response (Figure S4E). Similar to naloxone, CTAP significantly diminished food-induced suppression of AgRP neuron activity. Notably, naloxone and CTAP did not reduce the initial fast drop in AgRP neuron activity immediately after food access, which is thought to be mediated by sensory cues (Figure 4D). These results suggest that opioid signaling contributes to suppression of AgRP neurons induced by ongoing consumption, but not by sensory detection, of food.

Satiety hormones are thought to contribute to a sustained phase of AgRP neuron silencing after ingestion. Therefore, we next tested whether opioid signaling is required for suppression of AgRP neuron activity by peripheral satiety hormones. Consistent with earlier reports,[26,27] we found that i.p. injection of a cocktail of satiety hormones (CCK, PYY,

amylin) rapidly suppressed *in vivo* AgRP neuron activity, as determined by fiber photometry imaging. However, combined injection of these hormones with naloxone significantly reduced their inhibitory effect (Figures 4E and 4F). Conversely, ethanol-induced suppression of AgRP neurons was insensitive to naloxone co-administration (Figures 4G and 4H).[28] These findings suggest that opioid signaling contributes to food but not drug-induced suppression of AgRP neuron activity.

Suppressing AgRP neuron activity is known to diminish appetite.[29,30] Paradoxically, opioids are well known to increase appetite, particularly for palatable food. To resolve this, we next tested the impact of MOR activation on natural feeding at dark onset. Consistent with earlier AgRP neuron suppression studies, i.p. DAMGO injection at dark onset caused a small but significant decrease in food intake over the next 4 h. Remarkably, inline with a recent report,[31] administration of morphine, another MOR agonist with better brain access, caused much more robust appetite suppression (Figures 4I and 4J).

Food-dependent opioid surge acts through MOR on AgRP neurons

Our results from pharmacologic studies suggest that opioid signaling contributes to food-mediated AgRP neuron suppression and can reduce the consumed food amount. Because opioids have the capacity to reduce AgRP neuron activity both cell autonomously and non-cell autonomously, it remains unresolved whether it is the MORs on AgRP neurons per se or elsewhere that mediate these effects. To address this, we generated mice for AgRP-specific deletion of MOR expression (Figure 5A; *Agrpires-cre:Oprm1*$^{flox/flox}$, hereafter referred to as AgRP-MKO). We first functionally verified successful MOR deletion by performing loose seal recordings from fasted mice. Unlike wild-type controls (WT), bath application of DAMGO in the presence of synaptic blockers no longer caused any change in AgRP neuron activity in AgRP-MKO mice, demonstrating successful MOR ablation (Figures 5B and 5C). We next tested whether food-induced suppression is impaired in these mice, as would be anticipated from MOR antagonism experiments. We found that chow presentation after fasting caused a robust drop in AgRP neuron activity that was indistinguishable between AgRP-MKO mice and their WT littermates (Figure 5D). Similarly, the activity suppression induced by satiety hormones was also not affected in AgRP-MKO mice (Figure 5E). Notably, however, there was a transient trend toward a decrease in the amount of AgRP neuron activity suppression observed after palatable food presentation to freely feeding mice (Figure 5F).

The discrepancy between pharmacologic MOR blockage and AgRP neuron-selective MOR ablation could be due to a contribution of opioid receptors on other neurons. If this is the case, then MOR agonists would still be expected to modulate AgRP neuron activity even in AgRP-MKO mice. Although our slice recordings from AgRP-MKO mice ruled out any impact of direct MOR activation, the presence of synaptic blockers in these recordings could have masked indirect actions. Additionally, our ARC slices may not contain the entirety of opioid-sensitive circuit elements that can lead to indirect AgRP neuron suppression. To circumvent these caveats, we used *in vivo* fiber photometry imaging to test whether AgRP neurons in AgRP-MKO mice can still be suppressed by i.p. injection of MOR agonists. Remarkably, i.p. injection of morphine was still capable of strongly suppressing AgRP

neuron activity, albeit slightly less effective than in WT littermates (Figure 5G). This is in line with the observation that MOR agonism can suppress AgRP neuron activity both cell autonomously and indirectly through its network action. This also implies that MORs on AgRP neurons may not contribute to refeeding- or satiety hormone-mediated suppression of AgRP neurons, otherwise we would have seen a similar alleviation of suppression in AgRP-MKO mice. Instead, opioids might be acting primarily through upstream networks to suppress AgRP neurons in response to food or satiety hormones. If this is the case, then MOR antagonism in AgRP-MKO mice would still be expected to diminish food- and satiety hormone-mediated suppression. However, unlike WT mice, we found that, in AgRP-MKO mice, food and satiety hormone-mediated suppression cannot be alleviated by opioid receptor antagonists (Figures 5H and 5I). Taken together, these findings suggest that chow refeeding or satiety hormone-mediated opioid release contributes to AgRP neuron suppression cell autonomously; however, when AgRP neuronal MOR expression is ablated congenitally, this suppression is compensated by other transmitters.

AgRP-specific ablation of *Oprm1* alters diet preference

Based on somatic GCaMP-based measurements, the lack of MORs on AgRP neurons appears to be largely compensated via non-opioidergic mechanisms. However, we also showed that opioids have the capacity to suppress AgRP neuronal output from synaptic terminals (Figures 3D-3F), independent of their actions on soma. Whether these synaptic actions can be compensated in AgRP-MKO mice is unclear. Additionally, while experiments with pharmacologic doses of satiety hormones suggest normal AgRP neuron suppression, whether physiological doses during actual feeding are still effective is unclear. To address this, we next examined behavioral consequences of AgRP neuronal MOR deletion. We found that overall daily food intake and body weight were unaltered in AgRP-MKO mice (Figures 6A and 6B). Lack of MOR in AgRP neurons abolished the feeding-suppressing effect of DAMGO; however, morphine was still highly effective, suggesting that the latter can still act through non-AgRP neuronal opioid receptors (Figures 6C and 6D).

Given the selective but transient reduction trend in HFHS-mediated suppression of AgRP neurons in AgRP-MKO mice, we further dissected the impact on palatable food consumption. For this, we first quantified the amount of chow, high-fat, or high-sucrose diet consumption during refeeding. While AgRP-MKO mice consumed similar chow and high-sucrose diets, there was a transient increase in high-fat diet consumption (Figures 6E-6H), which is in line with the AgRP neuronal response to these diets from the same mice. To better dissect the high-fat diet (HFD) specificity of this effect, we provided mice with two feeders: one with chow and the other containing HFD pellets. We then let mice eat *ad libitum* for 2 days while monitoring their food preference. As expected, when given the choice, both AgRP-MKO mice and their WT littermates selectively opted for HFD pellets; however, HFD preference tended to be significantly higher in AgRP-MKO mice (Figures 6I-6K). Importantly, this was not due to increased reward by HFD because progressive ratio task after fasting gave similar break point results between AgRP-MKO and WT littermates (Figure 6L). These results suggest that MOR signaling on AgRP neurons may contribute to fat-induced satiety.

DISCUSSION

Opioids are known to promote reward-related feeding. Here, we found that opioidergic regulation of appetite extends to homeostatic hunger circuits. Contrary to its established orexigenic role, AgRP neuron opioid signaling restrains palatable food consumption and contributes to AgRP neuron suppression by ingestion and satiety hormones. These results suggest that opioids play a larger role in appetite regulation than previously acknowledged, extending to modulation of homeostatic hunger circuits with ingestion.

Previous biochemistry studies of rats show that palatable food increases CSF and circulating β-endorphin levels and increases MOR occupation in the mesolimbic pathway.[14,32,33] Consistently, our results using direct *in vivo* imaging with fluorescent opioid sensor showed that hypothalamic opioid levels are also highly responsive to feeding, including chow food, suggesting that feeding-related opioid signaling is neither exclusive to reward circuits nor to palatable food. These results are in line with a recent human imaging study showing an increased MOR binding PET signal throughout forebrain even with nonpalatable food after fasting.[34] Notably, hypothalamic opioid release was sensitive to the hunger state because chow presentation in mice with free food access did not cause any significant increase in the deltaLight signal. Moreover, ingestion was required for opioid release because inaccessible food presentation to fasted mice also did not increase the deltaLight signal. Taken together with the observation that the food-induced opioid signal does not peak until ~ 10 min into feeding, these findings suggest that post-ingestive processes could be more important for opioid release than sensory-mediated signals. This is further supported by the observation that the initial drop in AgRP neuron activity after food access was insensitive to opioid receptor antagonists, whereas later phases of suppression were diminished by them.

Studies primarily based on pharmacological manipulations established that opioids promote palatable food consumption. We propose that, contrary to its role in the mesolimbic pathway, opioid signaling in AgRP neurons conveys fat- and, to a lesser degree, chow-induced satiety signaling to reduce further consumption; however, the chow ingestion-mediated signal is sensitive to nutritional status and can be augmented by deprivation. Several lines of evidence support this conclusion. (1) HFD and chow food rapidly increased the deltaLight signal in the mediobasal hypothalamus (Figure 1). (2) Food- and satiety hormone-mediated suppression of AgRP neuron activity was attenuated by MOR antagonism (Figure 4). (3) MOR antagonism disinhibited AgRP neuron activity in acute slices prepared from fed but not fasted mice, suggesting tonic suppression (Figures 4 and S4). (4) mRNA levels for opioid peptides in the ARC[35] and MOR levels in AgRP neurons decrease by food restriction (Figure S4A). (5) Mice with AgRP-specific ablation of *Oprm1* showed increased fat preference, suggesting that MOR signaling normally restrains fat consumption (Figure 6). (6) DAMGO injection diminishes feeding at dark onset, an effect required AgRP specific MOR expression. (7) Further support for a satiety-inducing role of opioid signaling comes from β-endorphin knockout mice, which are hyperphagic and obese.[36] (8) Similarly, a rapid reduction in β-endorphin levels has been suggested to be an early marker for obesity predisposition in both humans and mice.[37] (9) Finally, hypothalamic neuron populations that are positioned to release endogenous opioids in the vicinity of AgRP neurons are rapidly activated by chow or palatable food.[11,13,38] ARC^{POMC} and DMH^{PDYN}

neurons have extensive axonal arborizations within the ARC. Moreover, due to opioid's capacity to suppress release from AgRP axon terminals, there might be other opioidergic neurons that do not directly project to the ARC but can still modulate AgRP neuronal output through their overlapping projections. Collectively, these observations suggest that food-induced opioid release onto AgRP neurons promotes satiation rather than appetizing further consumption.

Consistent with a recent report,[31] we also found suppression of dark-onset feeding by both DAMGO and morphine. Interestingly, morphine suppressed feeding much more robustly, and unlike DAMGO, this effect persisted even in AgRP-MKO mice. Morphine-induced AgRP neuron activity suppression was also largely intact in AgRP-MKO mice, suggesting that this was largely mediated by activation of opioid receptors located on non-AgRP neurons. The difference between DAMGO and morphine could be due to relatively poor permeability of DAMGO through the blood-brain barrier (~2,000-fold lower compared with morphine[39,40]), which is also thought to underlie its low antinociceptive potency despite its higher affinity. Given that the arcuate nucleus capillaries are highly fenestrated and have direct access to small-molecular-weight plasma proteins,[41-43] DAMGO may have selectively acted on ARC neurons or their local axon terminals, including AgRP-neurons, thereby making its effect sensitive to AgRP-selective MOR deletion, whereas morphine likely acts on broader circuits that DAMGO has poor access.

Divergent outcomes of pharmacologic MOR antagonism and AgRP-specific MOR ablation revealed that the contribution of MOR-dependent inhibition during refeeding can be largely compensated. Nevertheless, long-term diet preference was still significantly tilted toward an HFD in AgRP-MKO mice. These results also confirmed that refeeding- or satiety hormone-dependent activity suppression is contributed by stimulation of MORs directly located on AgRP neurons as opposed to MORs in the upstream networks because the sensitivity to MOR antagonists was abolished in AgRP-MKO mice. What then is the physiological role of opioidergic inhibition of AgRP neurons through upstream networks? One possibility is that these networks could be involved in stress or malaise response.

MOR downstream effectors have been extensively studied in the context of addiction and pain modulation. While β-arrestin is primarily known for desensitizing MOR signaling, a growing body of evidence suggests that it may also activate various intracellular effector pathways.[44,45] Remarkably, incomplete inhibition of G-protein cycling through a low concentration of pipette GDPβS sensitized DAMGO's hyperpolarizing effect to the blockers of GRK2/3 and PI3K, thereby revealing an intracellular β-arrestin-dependent pathway (MOR→GRK→β-arrestin→PI3K→K_{ATP}). Recently, it has been reported that β-arrestin→PI3K signaling works downstream of the IR and is required for rapid inhibition of AgRP neuron activity,[19,20] suggesting that MOR and IR downstream pathways may converge on these intracellular effectors to downregulate AgRP neuron function. It is unclear why inhibitors of the β-arrestin/PI3K pathway are effective only at a low dose of cytosolic GDPβS levels. One possibility could be that MOR complexes with distinct biochemical properties may have a nonoverlapping subcellular distribution so that those located close to the soma may not require β-arrestin for hyperpolarization as much as those on distal dendrites. Thus, low pipette GDPβS levels may still effectively block somatic MOR→G-

protein signaling and spare the distal ones that rely on the β-arrestin→PI3K pathway, which would be exposed to even lower GDPβS concentrations due to diffusion constraints. Alternatively, these MOR complexes might be organized into distinct microdomains with varying accessibility or sensitivity to G-protein blockers.[46] Regardless of the underlying mechanism, these results suggested a MOR downstream signaling pathway that is β-arrestin/PI3K sensitive and can rapidly hyperpolarize AgRP neurons to reduce further feeding (Figure 7).

Exogeneous opioid drugs are significantly more rewarding under food deprivation.[47-49] Cocaine- and morphine-induced conditioned place preference (CPP) is more robust and resistant to extinction in food-deprived mice.[50,51] Conversely, increased reward sensitivity in a deprived state is abolished by naloxone or CTAP treatment,[52,53] suggesting that food deprivation increases reward sensitivity through a MOR-dependent pathway. Notably, food restriction also drives negative valence through increased AgRP neuron activity, and its silencing by food access or chemogenetic manipulation is rewarding.[54,55] Thus, like food, MOR-dependent inhibition of AgRP neuron activity, as shown here, may contribute to increased opioid reward, especially under deprivation conditions. This would also suggest that AgRP neurons might be one of the targets of opioidergic drugs of abuse that contributes to its enhanced reward in a nutritional state-dependent manner. It is likely that this could be extended to other drugs of abuse, which has also been shown to suppress AgRP neuron activity.[28] Further support comes from the experiments in which, like hunger, chemogenetic modulation of AgRP neuron activity has been shown to alter nucleus accumbens (Nac) DA levels and VTA activity in response to food and drugs, and at least food-dependent DA release is sensitive to the obese state.[28,38,56,57] A plausible mechanism mediating this effect may involve direct AgRP neuronal projections to VTA and subsequent modulation of reward function;[58,59] however, midbrain independent pathways could also be involved.[60,61]

Diet-induced obesity blunts the responsiveness of AgRP neuron activity to food.[38,62] Taken together with our results, it is possible that dysregulated opioid signaling, as reported in obese subjects, may contribute to fat-induced desensitization of AgRP neurons, thereby impairing a crucial post-ingestive feedback signal to promote obesity. Future work will determine whether alterations in opioid signaling in this specific circuit node contribute to obesity and eating disorders.

Limitations of the study

Our study did not identify the source neurons for endogenous opioids that are released in response to food. As discussed above, there are several possible candidate neuron populations known to project to the ARC that are activated by feeding, including ARC^{POMC} and DMH^{PDYN}.

In a subset of our recordings that involve i.p. injections, we observed handling-dependent suppression of AgRP neuron activity. This is likely due to stress, which has been reported recently to suppress AgRP neurons.[63] However, we think this is unlikely to significantly affect our measurements because opioidergic signaling appears to build slowly over time, while stress-based suppression rapidly dissipates. Additionally, both control and

experimental groups underwent same types of handling procedures and would be expected to be affected similarly by handling.

STAR★METHODS

RESOURCE AVAILABILITY

Lead contact—Further information and requests for resources and reagents should be directed to and will be fulfilled by the lead contact, Deniz Atasoy (deniz-atasoy@uiowa.edu).

Materials availability—No materials have been generated in this study.

Data and code availability

- All data reported in this paper will be shared by the lead contract upon request.
- The custom script used for analysis is available from the lead contact upon request.
- Any additional information required to reanalyze the data reported in this paper is available from the lead contact upon request.

EXPERIMENTAL MODEL AND STUDY PARTICIPANT DETAILS

Mice—Mice were housed in home cages (12:12 light:dark cycle), having *ad libitum* access to standard chow food and water, unless stated otherwise. When required, animals were fasted for 18–24 h. Mouse lines *Agrp-ires-cre* (Agrp$^{tm1(cre)Lowl}$, Jackson Labs Stock 012899), *Npy-gfp* (Jackson Labs Stock 006417), Oprm$^{fl/fl}$ (Jackson Labs Stock 030074) were back-crossed with C57BL/6 (Jackson Labs Stock 000664) for maintenance. Studies were performed with 2–6 months old, age- and sex-matched male and female mice. Animal care and experimental procedures were approved by University of Iowa Animal Research Committee. Mice welfare and health checks were conducted in accordance with the Institutional Animal Care and Use Committee (IACUC) guidelines. Sentinel mice cages were periodically screened for pathogens. Mice that displayed unhealthy posture or more than 20% weight loss were removed from the study.

METHOD DETAILS

Stereotaxic surgeries and rAAV injections—Stereotaxic surgeries were performed as described previously.[64] Briefly, under anesthesia with 1.5% isoflurane in the stereotaxic instrument (David Kopf instruments, Tujunga-CA), scalp was incised to expose skull, a small hole was opened with a drill and 150 to 600 nL virus (pGP-AAV-CAG-FLEX-jGCaMP7s-WPRE (AAV1, Addgene 104495), AAV9-*syn*-deltaLight3.0[15] and AAV9-*syn*-delta-Light0[15] (Canadian Neurophotonics, sensor: 300nL of 3.3×10^{12} vg/mL and mutant sensor: 300nL of 9.5×10^{12} vg/mL respectively), AAV-CAG-GFP (AAV5, Addgene 37825), AAV-ChR2) was injected bilaterally and intracranially using a pulled glass pipette (Drummond Scientific, Wiretrol, Broomall-PA). Viral injections were performed in the ARC (bregma: −1.25 mm, midline: ±0.25 mm, dorsal surface: −5.6 mm) by a micromanipulator (Narishige, East Meadow, NY). Scalp was stitched, or ferrule placement was performed

after viral injections. For *in vivo* fiber photometry recording, ferrule capped metal optical fiber (200 μm core diameter, NA = 0.48, Thorlabs) was implanted above the ARC using the same coordinates, except for the dorsal surface, which was ~100–200 mm above the viral injection. Ferrules were fixed with dental cement. At least 2 weeks were given for animal recovery and transgene expression before further experiments.

***In vivo* imaging—**Following stereotaxic surgery recovery, animals were single housed in custom made plexiglass cages with free access to chow food and cotton bedding and were allowed for 1–2 days of acclimatization to the cage. Then, the mice were tethered to the fiber optic fiber (200 μm core, 0.48 NA, bundled fibers, Doric Lenses) using black ceramic mating sleeves. Signal from Ca^{2+} or opioid sensor imaging was recorded at 3Hz sampling rate, using Doric FP Bundle Imager (Doric Lenses), with light intensity (for 405 nm and 465 nm wave-length) of 30–50 μW. Food was removed during recording periods to prevent interference of food consumption related activity changes with the data. For the analysis, isosbestic signal (405nm) was fitted to the Ca^{2+}/sensor dependent (465 nm) signal using the linear least squares fit in a custom MATLAB script and ΔF/F was calculated as (465 nm – fitted 405 nm)/(fitted 405 nm). Then, z-scores were calculated using the mean and standard deviation of the baseline period (5–20 min before the intended event) to account for the inter-animal differences in signal intensities (Z score = $(F\text{-}F\mu_{(baseline)})/std_{(baseline)}$, where F is the 405 corrected 465 (ΔF/F), Fμ is the mean and std is the standard deviation of the baseline). For food presentation experiments, 465 signal was used for calculation of z-scores, instead of ΔF/F values. After the post hoc analysis, mice were eliminated by the off-target fiber tip location and virus or sensor expression.

Electrophysiology—Slice preparations were performed as described previously.[65] Briefly, P60-P90 mice were sacrificed brains were immersed in NMDG-HEPES aCSF cutting solution (in mM): 92 NMDG, 2.5 KCl, 1.25 NaH_2PO_4, 30 $NaHCO_3$, 20 HEPES, 25 glucose, 2 thiourea, 5 Na-ascorbate, 3 Na-pyruvate, 0.5 $CaCl_2$•$2H_2O$, and 10 $MgSO_4$•$7H_2O$. During slicing, the brain tissue is kept in 95% O2/5% CO2 aerated ice-cold cutting solution and 300 μm thick fresh slices containing the ARC were obtained with vibratome (Campden Instruments). The slices were then transferred to 95% O_2/5% CO_2 aerated and HEPES containing aCSF incubation solution containing (in mM): 92 NaCl, 2.5 KCl, 1.25 NaH_2PO_4, 30 $NaHCO_3$, 20 HEPES, 25 glucose, 2 thiourea, 5 Na-ascorbate, 3 Na-pyruvate, 2 $CaCl_2$·$2H_2O$, and 2 $MgSO_4$·$7H_2O$. Brain sections were incubated in this solution for >30 min and then transferred to the recording chamber which has the recording aCSF (in mM): 124 NaCl, 2.5 KCl, 1.25 NaH_2PO_4, 24 $NaHCO_3$, 12.5 glucose, 5 HEPES, 2 $CaCl_2$·$2H_2O$, and 2 $MgSO_4$·$7H_2O$.

AgRP/NPY neurons were targeted by fluorescence guided recordings from *Npy-gfp* mice. For loose seal and whole cell recordings electrodes with 4–5 MΩ tip resistances were used. For loose-seal recordings aCSF was used as the pipette solution. Presence of synaptic blockers were indicated for each experiment. If needed, the blockers CNQX (10 μM) + AP5 (50 μM) were added to block excitatory transmission and PTX (50 mM) was added to block $GABA_A$-receptors. For whole cell voltage-clamp recordings involving synaptic current measurements (Figure 3), pipette solution contained (in mM): 125 CsCl, 5 NaCl, 10

HEPES, 0.6 EGTA, 4 Mg-ATP, 0.3 Na_2GTP, 10 lidocaine N-ethyl bromide (QX-314), pH 7.35 and 290 mOsm. The holding potential was set to −60 mV. In whole cell configuration, 2–3 sweeps collected while photostimulating $ARC^{Agrp:ChR2}$ axons in PVN with 2 pulses at 10Hz delivered through objective. For whole cell current clamp recordings, pipette solution was based on potassium gluconate: (in mM): 145 K-gluconate, 1 MgCl2, 10 HEPES, 1.1 EGTA, 2 Mg-ATP, 0.5 Na2-GTP, and 5 Na_2-phosphocreatine (pH 7.3 with KOH; 290–295 mOsm). In a subset of experiments GTP was replaced by low (0.8 mM) or high (2.4 mM) concentration of GDPβS. MultiClamp 700B Amplifier (Molecular Devices, San Jose, CA) and Axon pCLAMP 11 software (Molecular Devices, San Jose, CA) were used to obtain and analyze data.

Behavior

Fasting – re-feeding assay: High-fat versus high-sucrose consumption was measured in control *Oprm*$^{fl/fl}$ and *Oprm*$^{-/-}$ mice using a back-to-back fasting-refeeding protocol. Mice were housed in home cages with an affixed FED3 feeding device (OpenEphys[66]) and were allowed to acclimate for 48 h prior to fasting. Mice were fasted for 24 h and subsequently re-fed either a high fat (27%, Bio-Serv #F07687) or high sucrose (94.8%, Bio-Serv #F07595) diet for 2 h. Consumption data were collected individually from mice for 2hrs after the mouse removed the first pellet from the dispense tray. After the 2 h re-feeding period, mice were fed normal chow (Bio-Serv #F0163) *ad libitum* for 48 h. Mice were then fasted for another 24 h period followed by a second re-feeding period (2 h). Diet treatments were intersubject counterbalanced across mice. The number of pellets consumed during the re-feeding trials were recorded and analyzed via two-way ANOVA with Bonferroni *post-hoc* adjustment.

Food preference test: Mice were single housed in home cages with 2 affixed FED3 devices, and were acclimated to the use of FED3 device for 2 days. Afterward, chow food in the second FED3 device was changed to HFD (Bioserv-F06245 diet with increased fat content, 22.7%), and food consumption in both feeders was recorded for 3 days. High fat preference was calculated as (number of HFD pellets)/(number of HFD + chow pellets)*100. We avoided using *Oprm*$^{fl/-}$ het mice as control since we observed significant increase in GFP injected het animals compared to uninjected control *Oprm*$^{fl/fl}$ mice (cntrl: 57.1 ± 6% vs. *Oprm*$^{fl/-}$:86 ± 3%, p = 0.0007). This could be due to surgery/injection or reduced MOR expression as a result of hypomorphism.

Progressive ratio task: After mice were acclimated to the use of FED3 devices, the FED3 setting was changed to ‘Fixed Ratio-1’ (FR1) mode, where mice had to poke their noses to one of the poker holes in the device to obtain food. After mice were acclimated to the use of FR1 mode for 2 days, the setting was changed to FR3 (3 pokes for one pellet). After 2 more days, mice were fasted and next day the device mode was set to progressive ratio schedule, that delivered HFD pellets with a nose poke ratio of 1, 2, 3, 5, 7, 9, 11, 14, 18, 22, etc. (modified from[67]). The break point was defined as the number of pellets where animals stopped working for more than 30 min.

Post hoc analysis—Mice were anesthetized and transcardially perfused with 4% paraformaldehyde (PFA) in phosphate buffer saline (0.1 M pH 7.4). Brains were collected, incubated in 4% PFA for 4 h and transferred to 30% sucrose for storage. Using a vibratome, 100 μm brain sections were collected and mounted with Fluoromount (Sigma F4680). When needed, immunostaining was performed with anti-GFP antibody to amplify signal (1:1000, Abcam Ab290) followed by mounting with Fluoromount (Sigma F4680). Imaging was performed by confocal microscopy (FV3000 Confocal Scanning Microscope, Olympus) and slide scanner microscope (VS200 Slide View, Olympus).

QUANTIFICATION AND STATISTICAL ANALYSIS

All results are represented as mean ± SEM for the indicated number of observations. Statistical details have been provided in the figures and figure legends. Differences between two groups were tested with two-tailed paired and unpaired Student's t-tests. For more than 2 groups, the statistical comparison was measured by one-way ANOVA using Prism 8.1 (GraphPad Software Inc.). N represents mice or neuron numbers as indicated for each experiment. A p value <0.05 was considered to be statistically significant.

Supplementary Material

Refer to Web version on PubMed Central for supplementary material.

ACKNOWLEDGMENTS

This work is supported by NIH R01DK126740 (to D.A.).

REFERENCES

1. Karlsson HK, Tuominen L, Tuulari JJ, Hirvonen J, Parkkola R, Helin S, Salminen P, Nuutila P, and Nummenmaa L (2015). Obesity is associated with decreased mu-opioid but unaltered dopamine D2 receptor availability in the brain. J. Neurosci 35, 3959–3965. [PubMed: 25740524]
2. Majuri J, Joutsa J, Johansson J, Voon V, Alakurtti K, Parkkola R, Lahti T, Alho H, Hirvonen J, Arponen E, et al. (2017). Dopamine and Opioid Neurotransmission in Behavioral Addictions: A Comparative PET Study in Pathological Gambling and Binge Eating. Neuropsychopharmacology 42, 1169–1177. [PubMed: 27882998]
3. Karlsson HK, Tuulari JJ, Tuominen L, Hirvonen J, Honka H, Parkkola R, Helin S, Salminen P, Nuutila P, and Nummenmaa L (2016). Weight loss after bariatric surgery normalizes brain opioid receptors in morbid obesity. Mol. Psychiatry 21, 1057–1062. [PubMed: 26460230]
4. Burghardt PR, Rothberg AE, Dykhuis KE, Burant CF, and Zubieta JK (2015). Endogenous Opioid Mechanisms Are Implicated in Obesity and Weight Loss in Humans. J. Clin. Endocrinol. Metab 100, 3193–3201. [PubMed: 26108093]
5. Tepper R, Weizman A, Apter A, Tyano S, and Beyth Y (1992). Elevated plasma immunoreactive beta-endorphin in anorexia nervosa. Clin. Neuropharmacol 15, 387–391. [PubMed: 1423337]
6. Daimon CM, and Hentges ST (2021). beta-endorphin differentially contributes to food anticipatory activity in male and female mice undergoing activity-based anorexia. Physiol. Rep 9, e14788. [PubMed: 33661571]
7. Daimon CM, and Hentges ST (2022). Inhibition of POMC neurons in mice undergoing activity-based anorexia selectively blunts food anticipatory activity without affecting body weight or food intake. Am. J. Physiol. Regul. Integr. Comp. Physiol 322, R219–R227. [PubMed: 35043681]
8. Brewerton TD, Lydiard RB, Laraia MT, Shook JE, and Ballenger JC (1992). CSF beta-endorphin and dynorphin in bulimia nervosa. Am. J. Psychiatry 149, 1086–1090. [PubMed: 1353317]

9. Peciña S, and Berridge KC (2005). Hedonic hot spot in nucleus accumbens shell: where do mu-opioids cause increased hedonic impact of sweetness? J. Neurosci 25, 11777–11786. [PubMed: 16354936]
10. Castro DC, Oswell CS, Zhang ET, Pedersen CE, Piantadosi SC, Rossi MA, Hunker AC, Guglin A, Morón JA, Zweifel LS, et al. (2021). An endogenous opioid circuit determines state-dependent reward consumption. Nature 598, 646–651. [PubMed: 34646022]
11. Chen Y, Lin YC, Kuo TW, and Knight ZA (2015). Sensory detection of food rapidly modulates arcuate feeding circuits. Cell 160, 829–841. [PubMed: 25703096]
12. Aponte Y, Atasoy D, and Sternson SM (2011). AGRP neurons are sufficient to orchestrate feeding behavior rapidly and without training. Nat. Neurosci. 14, 351–355. [PubMed: 21209617]
13. Garfield AS, Shah BP, Burgess CR, Li MM, Li C, Steger JS, Madara JC, Campbell JN, Kroeger D, Scammell TE, et al. (2016). Dynamic GABAergic afferent modulation of AgRP neurons. Nat. Neurosci 19, 1628–1635. [PubMed: 27643429]
14. Mizushige T, Saitoh K, Manabe Y, Nishizuka T, Taka Y, Eguchi A, Yoneda T, Matsumura S, Tsuzuki S, Inoue K, and Fushiki T (2009). Preference for dietary fat induced by release of beta-endorphin in rats. Life Sci. 84, 760–765. [PubMed: 19296904]
15. Tian L, Dong C, Gowrishankar R, Jin Y, He X, Gupta A, Wang H, Atasoy N, Flores-Garcia R, and Mahe K (2023). Unlocking opioid neuropeptide dynamics with genetically-encoded biosensors.
16. Betley JN, Xu S, Cao ZFH, Gong R, Magnus CJ, Yu Y, and Sternson SM (2015). Neurons for hunger and thirst transmit a negative-valence teaching signal. Nature 521, 180–185. [PubMed: 25915020]
17. Broberger C, Johansen J, Johansson C, Schalling M, and Hökfelt T (1998). The neuropeptide Y/agouti gene-related protein (AGRP) brain circuitry in normal, anorectic, and monosodium glutamate-treated mice. Proc. Natl. Acad. Sci. USA 95, 15043–15048. [PubMed: 9844012]
18. Erdtmann-Vourliotis M, Mayer P, Ammon S, Riechert U, and Höllt V (2001). Distribution of G-protein-coupled receptor kinase (GRK) isoforms 2, 3, 5 and 6 mRNA in the rat brain. Brain Res. Mol. Brain Res 95, 129–137. [PubMed: 11687284]
19. Könner AC, Janoschek R, Plum L, Jordan SD, Rother E, Ma X, Xu C, Enriori P, Hampel B, Barsh GS, et al. (2007). Insulin action in AgRP-expressing neurons is required for suppression of hepatic glucose production. Cell Metab. 5, 438–449. [PubMed: 17550779]
20. Pydi SP, Cui Z, He Z, Barella LF, Pham J, Cui Y, Oberlin DJ, Egritag HE, Urs N, Gavrilova O, et al. (2020). Beneficial metabolic role of beta-arrestin-1 expressed by AgRP neurons. Sci. Adv 6, eaaz1341. [PubMed: 32537493]
21. Yang Y, Atasoy D, Su HH, and Sternson SM (2011). Hunger states switch a flip-flop memory circuit via a synaptic AMPK-dependent positive feedback loop. Cell 146, 992–1003. [PubMed: 21925320]
22. Atasoy D, Aponte Y, Su HH, and Sternson SM (2008). A FLEX switch targets Channelrhodopsin-2 to multiple cell types for imaging and long-range circuit mapping. J. Neurosci 28, 7025–7030. [PubMed: 18614669]
23. Atasoy D, Betley JN, Li WP, Su HH, Sertel SM, Scheffer LK, Simpson JH, Fetter RD, and Sternson SM (2014). A genetically specified connectomics approach applied to long-range feeding regulatory circuits. Nat. Neurosci 17, 1830–1839. [PubMed: 25362474]
24. Rau AR, and Hentges ST (2017). The Relevance of AgRP Neuron-Derived GABA Inputs to POMC Neurons Differs for Spontaneous and Evoked Release. J. Neurosci. 37, 7362–7372. [PubMed: 28667175]
25. Henry FE, Sugino K, Tozer A, Branco T, and Sternson SM (2015). Cell type-specific transcriptomics of hypothalamic energy-sensing neuron responses to weight-loss. Elife 4, e09800. [PubMed: 26329458]
26. Su Z, Alhadeff AL, and Betley JN (2017). Nutritive, Post-ingestive Signals Are the Primary Regulators of AgRP Neuron Activity. Cell Rep. 21, 2724–2736. [PubMed: 29212021]
27. Beutler LR, Chen Y, Ahn JS, Lin YC, Essner RA, and Knight ZA (2017). Dynamics of Gut-Brain Communication Underlying Hunger. Neuron 96, 461–475.e5. [PubMed: 29024666]

28. Alhadeff AL, Goldstein N, Park O, Klima ML, Vargas A, and Betley JN (2019). Natural and Drug Rewards Engage Distinct Pathways that Converge on Coordinated Hypothalamic and Reward Circuits. Neuron 103, 891–908.e6. [PubMed: 31277924]
29. Siemian JN, Arenivar MA, Sarsfield S, and Aponte Y (2021). Hypothalamic control of interoceptive hunger. Curr. Biol 31, 3797–3809.e5. [PubMed: 34273280]
30. Krashes MJ, Koda S, Ye C, Rogan SC, Adams AC, Cusher DS, Maratos-Flier E, Roth BL, and Lowell BB (2011). Rapid, reversible activation of AgRP neurons drives feeding behavior in mice. J. Clin. Invest 121, 1424–1428. [PubMed: 21364278]
31. Laing BT, Jayan A, Erbaugh LJ, Park AS, Wilson DJ, and Aponte Y (2022). Regulation of body weight and food intake by AGRP neurons during opioid dependence and abstinence in mice. Front. Neural Circuits 16, 977642. [PubMed: 36110920]
32. Dum J, Gramsch C, and Herz A (1983). Activation of hypothalamic beta-endorphin pools by reward induced by highly palatable food. Pharmacol. Biochem. Behav 18, 443–447.
33. Colantuoni C, Schwenker J, McCarthy J, Rada P, Ladenheim B, Cadet JL, Schwartz GJ, Moran TH, and Hoebel BG (2001). Excessive sugar intake alters binding to dopamine and mu-opioid receptors in the brain. Neuroreport 12, 3549–3552. [PubMed: 11733709]
34. Tuulari JJ, Tuominen L, de Boer FE, Hirvonen J, Helin S, Nuutila P, and Nummenmaa L (2017). Feeding Releases Endogenous Opioids in Humans. J. Neurosci 37, 8284–8291. [PubMed: 28747384]
35. Kim EM, Welch CC, Grace MK, Billington CJ, and Levine AS (1996). Chronic food restriction and acute food deprivation decrease mRNA levels of opioid peptides in arcuate nucleus. Am. J. Physiol 270, R1019–R1024. [PubMed: 8928900]
36. Appleyard SM, Hayward M, Young JI, Butler AA, Cone RD, Rubinstein M, and Low MJ (2003). A role for the endogenous opioid beta-endorphin in energy homeostasis. Endocrinology 144, 1753–1760. [PubMed: 12697680]
37. Souza GFP, Solon C, Nascimento LF, De-Lima-Junior JC, Nogueira G, Moura R, Rocha GZ, Fioravante M, Bobbo V, Morari J, et al. (2016). Defective regulation of POMC precedes hypothalamic inflammation in diet-induced obesity. Sci. Rep 6, 29290. [PubMed: 27373214]
38. Mazzone CM, Liang-Guallpa J, Li C, Wolcott NS, Boone MH, Southern M, Kobzar NP, Salgado I.d.A., Reddy DM, Sun F, et al. (2020). High-fat food biases hypothalamic and mesolimbic expression of consummatory drives. Nat. Neurosci 23, 1253–1266. [PubMed: 32747789]
39. Fiori A, Cardelli P, Negri L, Savi MR, Strom R, and Erspamer V (1997). Deltorphin transport across the blood-brain barrier. Proc. Natl. Acad. Sci. USA 94, 9469–9474. [PubMed: 9256506]
40. Lindqvist A, Rip J, Gaillard PJ, Björkman S, and Hammarlund-Udenaes M (2013). Enhanced brain delivery of the opioid peptide DAMGO in glutathione pegylated liposomes: a microdialysis study. Mol. Pharm 10, 1533–1541. [PubMed: 22934681]
41. Ciofi P. (2011). The arcuate nucleus as a circumventricular organ in the mouse. Neurosci. Lett 487, 187–190. [PubMed: 20951768]
42. Faouzi M, Leshan R, Björnholm M, Hennessey T, Jones J, and Münzberg H (2007). Differential accessibility of circulating leptin to individual hypothalamic sites. Endocrinology 148, 5414–5423. [PubMed: 17690165]
43. Morita S, and Miyata S (2013). Accessibility of low-molecular-mass molecules to the median eminence and arcuate hypothalamic nucleus of adult mouse. Cell Biochem. Funct 31, 668–677. [PubMed: 23348371]
44. Al-Hasani R, and Bruchas MR (2011). Molecular mechanisms of opioid receptor-dependent signaling and behavior. Anesthesiology 115, 1363–1381. [PubMed: 22020140]
45. Che T, and Roth BL (2023). Molecular basis of opioid receptor signaling. Cell 186, 5203–5219. [PubMed: 37995655]
46. Kumar GA, and Puthenveedu MA (2022). Diversity and specificity in location-based signaling outputs of neuronal GPCRs. Curr. Opin. Neurobiol 76, 102601. [PubMed: 35797808]
47. Carr KD (2002). Augmentation of drug reward by chronic food restriction: behavioral evidence and underlying mechanisms. Physiol. Behav 76, 353–364. [PubMed: 12117572]
48. Cassidy RM, and Tong Q (2017). Hunger and Satiety Gauge Reward Sensitivity. Front. Endocrinol 8, 104.

49. Carr KD, and Wolinsky TD (1993). Chronic food restriction and weight loss produce opioid facilitation of perifornical hypothalamic self-stimulation. Brain Res. 607, 141–148. [PubMed: 8481792]
50. Zheng D, Cabeza de Vaca S, and Carr KD (2012). Food restriction increases acquisition, persistence and drug prime-induced expression of a cocaine-conditioned place preference in rats. Pharmacol. Biochem. Behav 100, 538–544. [PubMed: 22074687]
51. Jung C, Rabinowitsch A, Lee WT, Zheng D, de Vaca SC, and Carr KD (2016). Effects of food restriction on expression of place conditioning and biochemical correlates in rat nucleus accumbens. Psychopharmacology (Berl) 233, 3161–3172. [PubMed: 27376947]
52. Carr KD (1996). Feeding, drug abuse, and the sensitization of reward by metabolic need. Neurochem. Res 21, 1455–1467. [PubMed: 8947935]
53. Carr KD, and Papadouka V (1994). The role of multiple opioid receptors in the potentiation of reward by food restriction. Brain Res. 639, 253–260. [PubMed: 8205479]
54. Betley JN, Xu S, Cao ZFH, Gong R, Magnus CJ, Yu Y, and Sternson SM (2015). Neurons for hunger and thirst transmit a negative-valence teaching signal. Nature 521, 180–185. [PubMed: 25915020]
55. Chen Y, Lin YC, Zimmerman CA, Essner RA, and Knight ZA (2016). Hunger neurons drive feeding through a sustained, positive rein-forcement signal. Elife 5, e18640. [PubMed: 27554486]
56. Willmore L, Minerva AR, Engelhard B, Murugan M, McMannon B, Oak N, Thiberge SY, Peña CJ, and Witten IB (2023). Overlapping representations of food and social stimuli in VTA dopamine neurons. Pre-print at bioRxiv. 2023.05.17.541104.
57. Grove JCR, Gray LA, La Santa Medina N, Sivakumar N, Ahn JS, Corpuz TV, Berke JD, Kreitzer AC, and Knight ZA (2022). Dopamine subsystems that track internal states. Nature 608, 374–380. [PubMed: 35831501]
58. Stutz B, Waterson MJ, Šestan-Peša M, Dietrich MO, Škarica M, Sestan N, Racz B, Magyar A, Sotonyi P, Liu ZW, et al. (2022). AgRP neurons control structure and function of the medial prefrontal cortex. Mol. Psychiatry 27, 3951–3960. [PubMed: 35906488]
59. Dietrich MO, Bober J, Ferreira JG, Tellez LA, Mineur YS, Souza DO, Gao XB, Picciotto MR, Araújo I, Liu ZW, and Horvath TL (2012). AgRP neurons regulate development of dopamine neuronal plasticity and nonfood-associated behaviors. Nat. Neurosci 15, 1108–1110. [PubMed: 22729177]
60. Koch M, Varela L, Kim JG, Kim JD, Hernández-Nuño F, Simonds SE, Castorena CM, Vianna CR, Elmquist JK, Morozov YM, et al. (2015). Hypothalamic POMC neurons promote cannabinoid-induced feeding. Nature 519, 45–50. [PubMed: 25707796]
61. Rossi MA, and Stuber GD (2018). Overlapping Brain Circuits for Homeostatic and Hedonic Feeding. Cell Metab. 27, 42–56. [PubMed: 29107504]
62. Beutler LR, Corpuz TV, Ahn JS, Kosar S, Song W, Chen Y, and Knight ZA (2020). Obesity causes selective and long-lasting desensitization of AgRP neurons to dietary fat. Elife 9, e55909. [PubMed: 32720646]
63. de Araujo Salgado I, Li C, Burnett CJ, Rodriguez Gonzalez S, Becker JJ, Horvath A, Earnest T, Kravitz AV, and Krashes MJ (2023). Toggling between food-seeking and self-preservation behaviors via hypothalamic response networks. Neuron 111, 2899–2917.e6. [PubMed: 37442130]
64. Aklan I, Sayar Atasoy N, Yavuz Y, Ates T, Coban I, Koksalar F, Filiz G, Topcu IC, Oncul M, Dilsiz P, et al. (2020). NTS Catecholamine Neurons Mediate Hypoglycemic Hunger via Medial Hypothalamic Feeding Pathways. Cell Metab. 31, 313–326.e5. [PubMed: 31839488]
65. Ting JT, Lee BR, Chong P, Soler-Llavina G, Cobbs C, Koch C, Zeng H, and Lein E (2018). Preparation of Acute Brain Slices Using an Optimized N-Methyl-D-glucamine Protective Recovery Method. J. Vis. Exp 26, 53825.
66. Matikainen-Ankney BA, Earnest T, Ali M, Casey E, Wang JG, Sutton AK, Legaria AA, Barclay KM, Murdaugh LB, Norris MR, et al. (2021). An open-source device for measuring food intake and operant behavior in rodent home-cages. Elife 10, e66173. [PubMed: 33779547]
67. Richardson NR, and Roberts DC (1996). Progressive ratio schedules in drug self-administration studies in rats: a method to evaluate reinforcing efficacy. J. Neurosci. Methods 66, 1–11. [PubMed: 8794935]

Highlights

- Feeding increases mediobasal hypothalamic opioid levels
- AgRP neurons and their synapses are directly and indirectly inhibited by MOR agonists
- Opioid signaling contributes to AgRP neuron inhibition by feeding
- Selective ablation of MOR from AgRP neurons increases relative fat preference

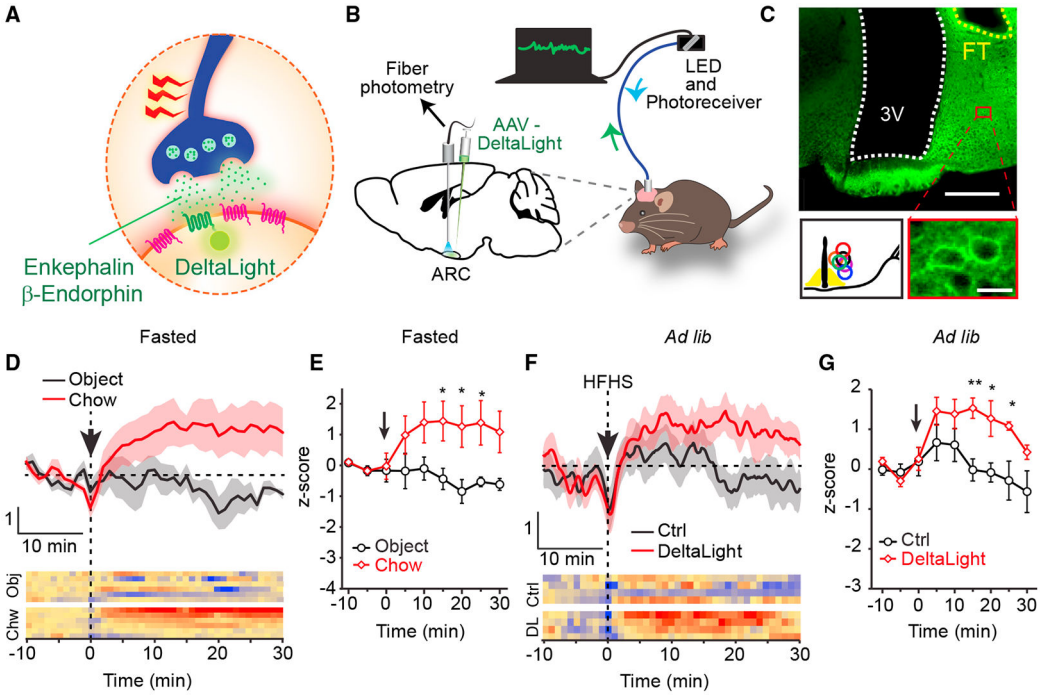

Figure 1. Feeding increases mediobasal hypothalamic opioid levels

(A) Cartoon depiction of the fluorescent sensor based on the δ-opioid receptor (DOR).

(B) Schematic showing injection of the DeltaLight sensor expressing virus into the arcuate nucleus and recording by fiber photometry.

(C) Photomicrograph showing ferrule placement (ferrule tip [FT]) over the mediobasal hypothalamus (top) and DeltaLight sensor expression in hypothalamic neurons (bottom right) and a map of FT locations in each mouse (bottom left). Scale bars: 200 μm (top), 30 μm (bottom right).

(D and E) Change in DeltaLight sensor activity in response to non-edible object and food presentation to overnight-fasted mice (D) and summarized mean sensor activity in 5-min time bins (E) (n = 6 mice, object vs. chow, paired t test, *p < 0.038).

(F and G) Change in DeltaLight and mutant sensor (Ctrl) activity in response to high fat, high sugar (HFHS) presentation in *ad libitum*-fed mice (F) and summarized mean sensor activity in 5-min bins (G) (n = 4 mice each, *p < 0.037, **p = 0.006, Ctrl vs. DeltaLight, unpaired t test).

All data are shown as mean ± SEM.

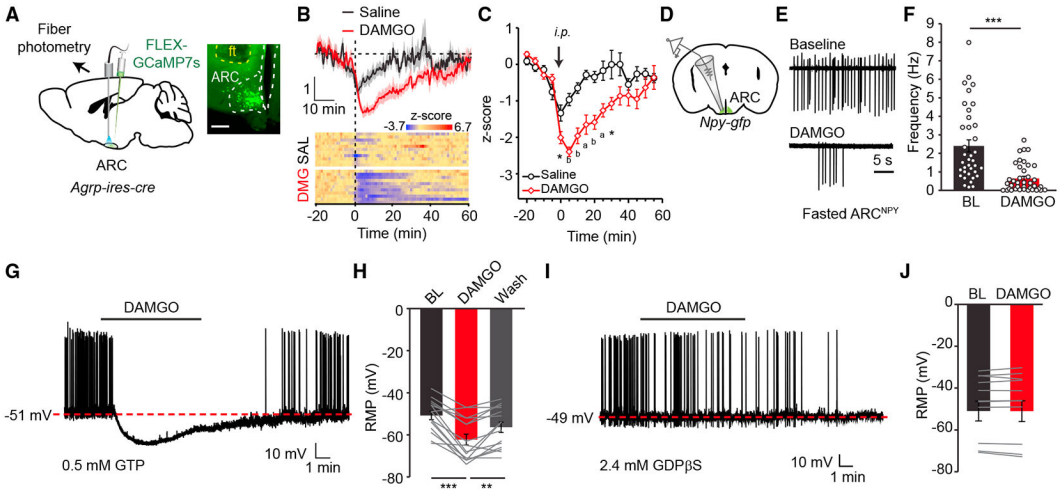

Figure 2. MOR activation rapidly suppresses AgRP neurons

(A) Schematic showing injection of the FLEX-GCaMP7s-expressing virus and ferrule placement over the ARC for fiber photometry recording and micrograph image showing injection and ferrule locations. Scale bar: 150 μm.

(B and C) Change in average AgRP neuron activity (B, top) and activity heatmap for individual mice (B, bottom) in response to i.p. injection (vertical dashed line) of saline or DAMGO (1 mg/kg) and summarized mean of AgRP neuron activity in 5-min time bins (C, n = 10 mice, *p < 0.043, [a]p<0.0084, [b]p<0.00011, saline vs. DAMGO, paired t test).

(D) Schematic showing loose seal recordings from GFP-labeled NPY neurons in the ARC.

(E and F) Representative loose seal traces (E) and summary of mean frequency of the recorded neurons (F) before (baseline) or after DAMGO (2 μM) bath application (n = 37–39 neurons, respectively/4 mice each, p < 0.0001, unpaired t test).

(G and H) Representative whole-cell current-clamp recording from ARC^{NPY} neurons (G) and resting membrane potential values (H) showing robust hyperpolarization by DAMGO in the presence of synaptic blockers (n = 15 neurons/3 mice, **p < 0.01, ***p < 0.001, paired t test).

(I and J) Whole-cell current-clamp recordings from ARC^{NPY} neurons using internal pipette solution with GDPβS instead of GTP with synaptic blockers (n = 11 neurons/3 mice).

All data are shown as mean ± SEM.

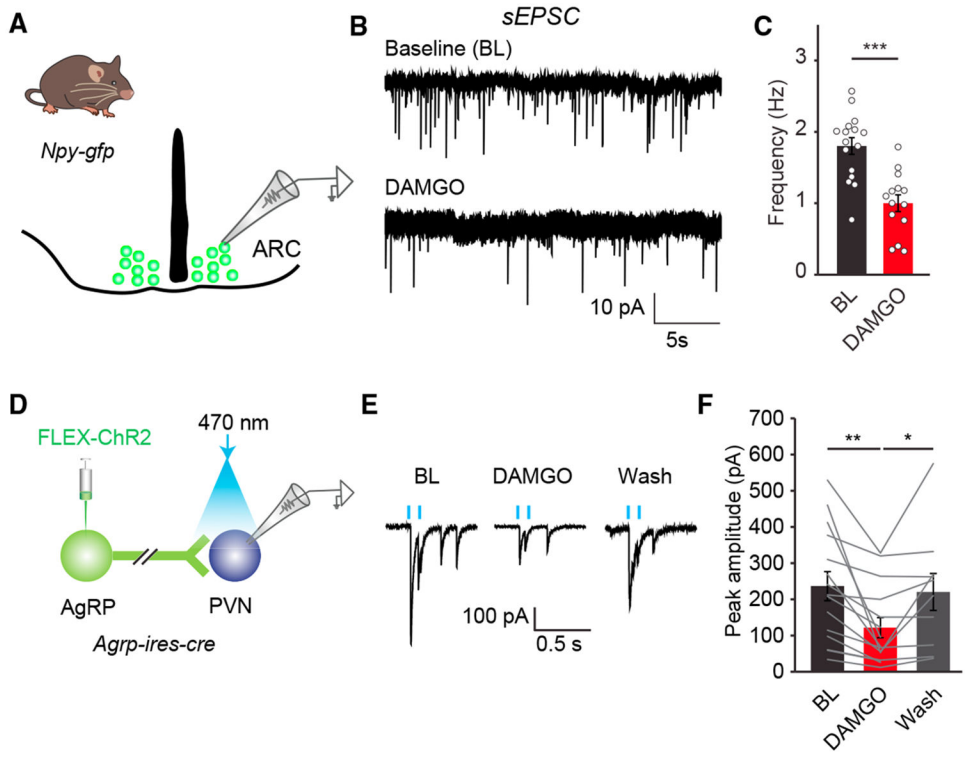

Figure 3. MOR signaling suppresses AgRP neuron input and output synapses

(A–C) Schematic showing recording from GFP-positive cells of *Npy-gfp* mice (A), representative whole-cell voltage-clamp traces showing DAMGO-mediated suppression of sEPSCs onto ARC^{NPY} neurons (B), and summary bar graph showing quantification (C) (n = 16 and 14 neurons/3 mice, $p < 0.001$, unpaired t test).

(D–F) Schematic showing identification of AgRP synaptic connection onto PVN neurons (D), representative whole-cell voltage-clamp recording traces from a PVN neuron receiving AgRP synaptic input and the impact of DAMGO on connection strength (E), and summary quantification (F) (n = 14 neurons/3 mice, *$p < 0.05$, **$p < 0.01$, paired t test).

All data are shown as mean ± SEM.

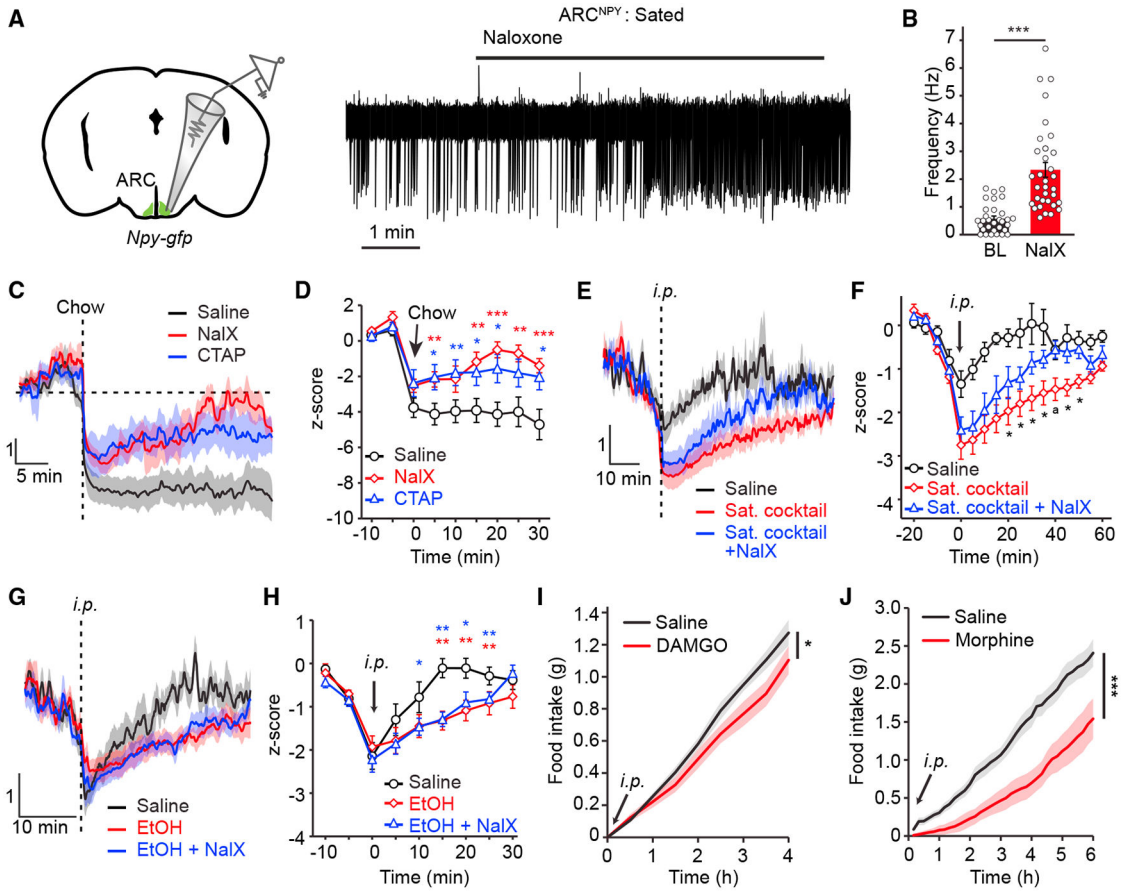

Figure 4. MOR signaling contributes to food-induced AgRP neuron suppression

(A and B) Schematic showing recording from GFP-positive cells of *Npy-gfp* mice, representative loose seal recording (A) and summary bar graph of firing rates (B) showing the effect of naloxone (NalX; 2 μM) treatment on ARC^{NPY} neurons in sated mice (n = 31–34 neurons/4 mice, $p < 0.0001$, unpaired t test).

(C and D) *In vivo* fiber photometry recording from AgRP neurons in fasted mice injected with saline, NalX (4 mg/kg), or CTAP (1.5 mg/kg) 15 min before chow presentation (vertical dashed line, C) and summary graph showing average change in activity in 5-min time bins (D) (n = 10 mice, *p < 0.05, **p < 0.0097, ***p < 0.00095; red asterisks, NalX vs. saline; blue asterisks, CTAP vs. saline; paired t test).

(E and F) *In vivo* fiber photometry recording from AgRP neurons in *ad-libitum*-fed mice injected with saline (from Figure 2B), satiety cocktail (3 μg/kg CCK + 10 μg/kg amylin + 10 μg/kg PYY) or satiety cocktail with NalX (vertical dashed line, E), and summary graph showing average change in activity in 5-min time bins (F) (n = 9 mice, satiety cocktail vs. satiety cocktail with NalX, paired t test, *p < 0.04, $^{a}p = 0.0084$).

(G and H) *In vivo* fiber photometry recording from AgRP neurons in *ad libitum*-fed mice injected with saline, EtOH (15%), or EtOH with NalX (vertical dashed line, G) and summary graph showing average change in activity in 5-min time bins (H) (n = 8 mice; red asterisks, saline vs. EtOH; blue asterisks, saline vs. EtOH with NalX; paired t test, **p < 0.0095, *p < 0.019).

(I and J) DAMGO-induced (I) and morphine-induced (J) suppression of dark-onset feeding (*p = 0.033, ***p < 0.0001, paired t test).

All data are shown as mean ± SEM.

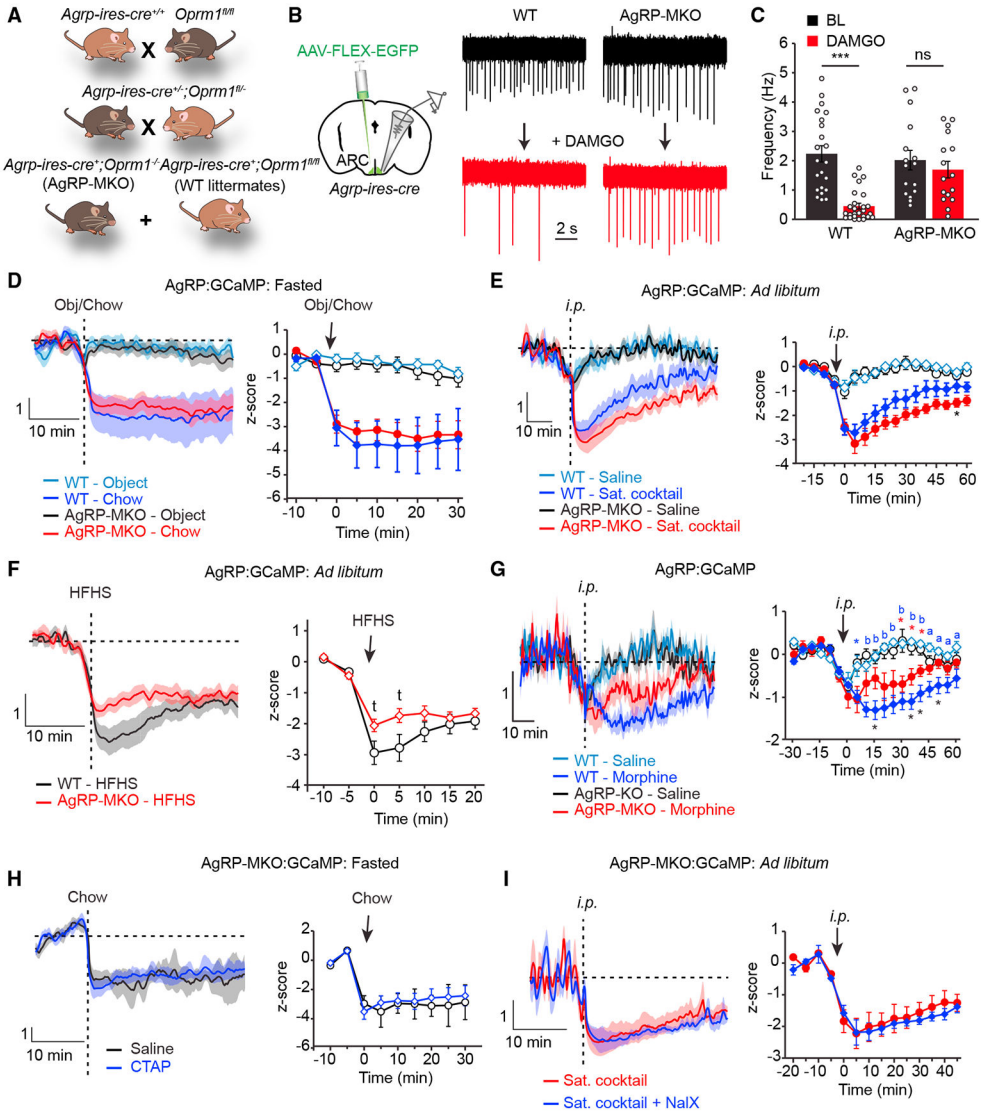

Figure 5. Congenital loss of *Oprm1* in AgRP neurons is largely compensated by non-opioidergic mechanisms

(A) Breeding strategy to generate mice with AgRP neuron-specific ablation of MOR.

(B and C) Schematic showing recording from GFP-positive cells in cre-dependent GFP-expressing virus-injected *Agrp-ires-cre* mice and representative loose seal traces showing effect of DAMGO perfusion in WT and MOR-deficient (AgRP-MKO) AgRP neurons' firing rates (B) and summary bar graph showing quantification (C). WT, 22–26 neurons; AgRP-MKO, 16 neurons each for BL and DAMGO recordings, respectively. BL vs. DAMGO, unpaired t test, ***p < 0.001; ns, not significant).

(D) *In vivo* fiber photometry recording from AgRP neurons in fasted WT and AgRP-MKO mice during object or chow presentation (vertical dashed line, left) and summary graph showing average change in activity in 5-min time bins (right) (n = 9 WT, 10 AgRP-MKO mice; all time points: not significant for WT vs. AgRP-MKO comparisons; unpaired t test).

(E) *In vivo* fiber photometry recording from AgRP neurons in *ad libitum*-fed WT and AgRP-MKO mice injected with saline or satiety cocktail (vertical dashed line, left) and

summary graph showing average change in activity in 5-min time bins (right) (n = 10 mice each, WT vs. AgRP-MKO, unpaired t test, *p = 0.047).

(F) *In vivo* fiber photometry recording from AgRP neurons in *ad libitum*-fed WT and AgRP-MKO mice during HFHS presentation (vertical dashed line, left) and summary graph showing average change in activity in 5-min time bins (right) (n = 11 WT, 9 AgRP-MKO mice; t, trend; p < 0.07, unpaired t test).

(G) *In vivo* fiber photometry recording from AgRP neurons in *ad libitum*-fed WT and AgRP-MKO mice injected with saline or morphine (10 mg/kg, vertical dashed line, left) and summary graph showing average change in activity in 5-min time bins (right) (n = 11 WT, 9 AgRP MKO mice; WT morphine vs. AgRP-MKO morphine, unpaired t test, black *p < 0.046; blue marks, WT; red marks, AgRP-MKO; saline vs. morphine paired t tests, *p < 0.043, ap<0.0091, bp<0.001).

(H) *In vivo* fiber photometry recording from AgRP neurons in fasted AgRP-MKO mice during chow presentation (vertical dashed line, left) after i.p. injection of saline and CTAP and summary graph showing average change in activity in 5-min time bins (right) (n = 3 mice, all time points: not significant, paired t test).

(I) *In vivo* fiber photometry recording from AgRP neurons in *ad libitum*-fed AgRP MKO mice during i.p. injection of satiety cocktail with and without NalX (vertical dashed line, left) and summary graph showing average change in activity in 5-min time bins (right) (n = 3 mice, all time points: not significant, paired t test).

All data are shown as mean ± SEM.

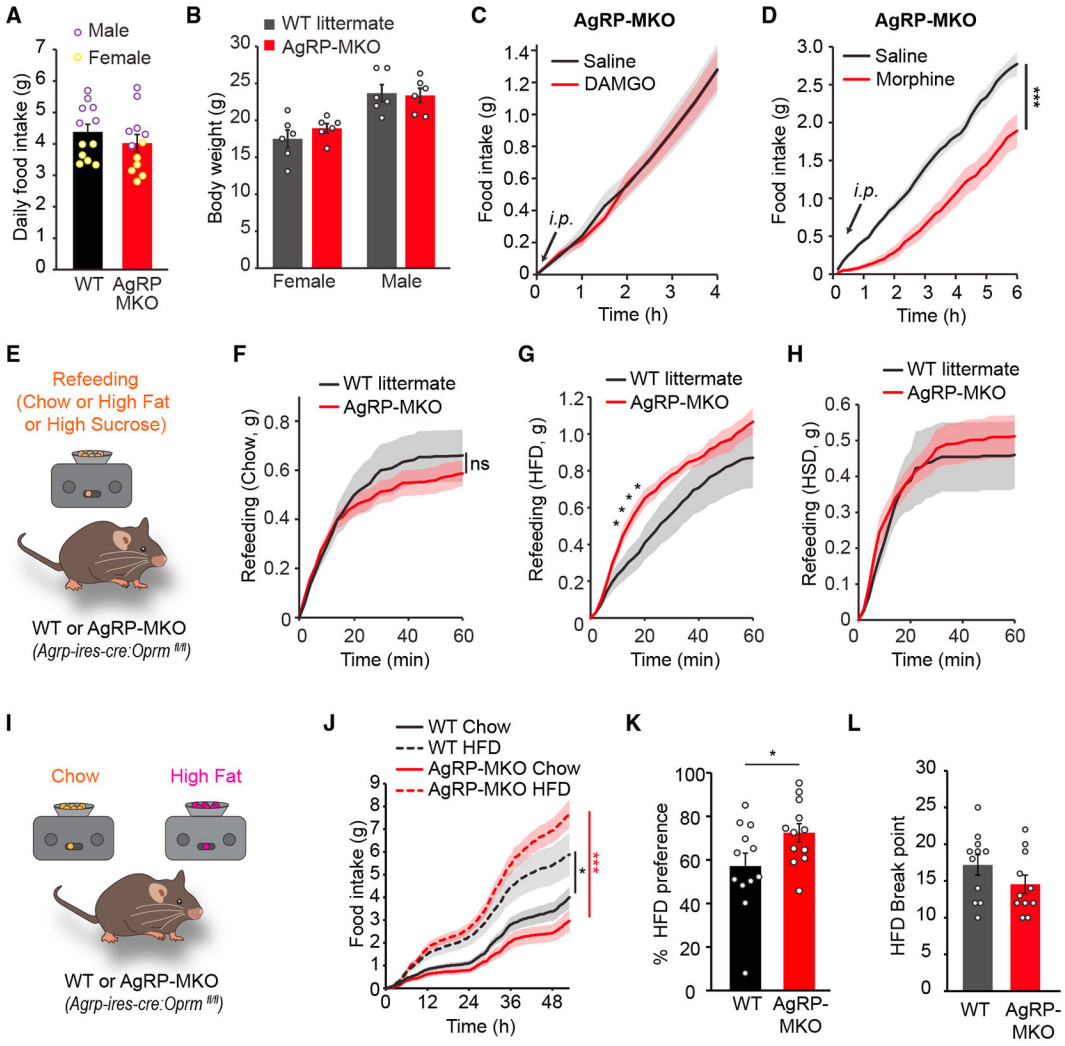

Figure 6. AgRP neuron-specific ablation of *Oprm1* alters diet preference by selectively reducing fat satiety

(A and B) Cumulative daily food intake (A) and body weight (B) of wild-type (WT) and AgRP-specific MOR knockout (AgRP-MKO) animals.

(C and D) Effect of DAMGO (C) and morphine (D) injections on dark-onset feeding in AgRP-MKO mice (***$p < 0.001$, unpaired t test).

(E) Schematic depicting the refeeding experiments in (F)–(H).

(F–H) Comparison of food consumption in WT and AgRP-MKO mice after overnight fasting when they were presented with chow (n = 12 each, unpaired t test; F), high-fat diet (HFD; n = 8 WT, 10 AgRP-MKO, *$p < 0.05$, unpaired t test; G), or high-sucrose diet (HSD; n = 8 WT, 10 AgRP-MKO, unpaired t test; H).

(I) Schematic depicting the experiment where mice have simultaneous *ad libitum* access to chow food and HFD.

(J) HFD and chow consumption in WT and AgRP-MKO animals for 2 days (n = 12 each, one-way ANOVA of the area under the curve with Tukey's correction for multiple comparisons, *$p = 0.048$, ***$p < 0.0001$).

(K) Preference for HFD as percentage of total daily food intake amount (chow + HFD, n = 12 each, unpaired t test, p = 0.047).
(L) Comparison of progressive ratio task break points (10 min of inactivity) to obtain HFD pellets in WT and AgRP-MKO mice after overnight fasting (n = 11 WT, 11 AgRP-MKO). All data are shown as mean ± SEM.

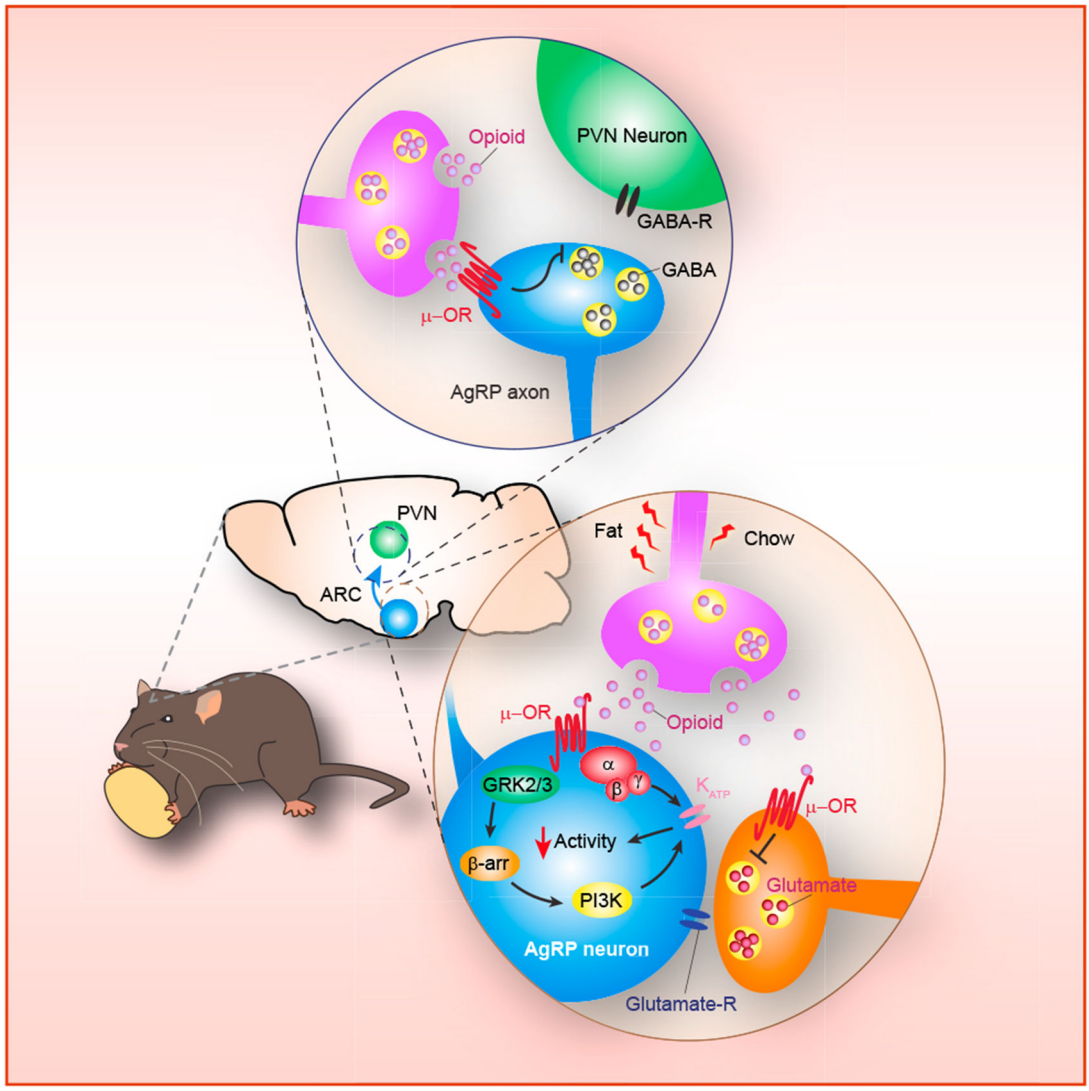

Figure 7. Opioidergic modulation of AgRP neuron activity

Food-dependent opioid release contributes to AgRP neuron suppression through cell-autonomous and network-level mechanisms.

KEY RESOURCES TABLE

REAGENT or RESOURCE	SOURCE	IDENTIFIER
Antibodies		
anti-GFP	Abcam	Cat#Ab290; RRID:AB_303395
Bacterial and virus strains		
AAV9-*syn*-deltaLight3.0	Canadian Neurophotonics	N/A
AAV9-*syn*-deltaLight0	Canadian Neurophotonics	N/A
AAV-CAG-GFP (AAV5)	Addgene	Cat#37825
AAV-EF1a-double floxed-hChR2(H134R)-EYFP-WPRE-HGHpA (AAV5)	Addgene	Cat#20298
pGP-AAV1-CAG-FLEX-jGCaMP7s-WPRE	Addgene	Cat#104495
Chemicals, peptides, and recombinant proteins		
SNC162	Tocris	Cat#1529
Naloxone hydrochloride dihydrate	Sigma-Aldrich	Cat#N7758
CTAP	Tocris	Cat#1560
DAMGO	Tocris	Cat#1171
Morphine	Sigma-Aldrich	Cat#M8777
CCK Octapeptide, sulfated	Tocris	Cat#1166
Peptide YY	Tocris	Cat#1618
Amylin	Tocris	Cat#3418
EtOH	Sigma	Cat#E7023
Experimental models: Organisms/strains		
Mouse: WT/Agrp-ires-cre: $Agrp^{tm1(cre)Lowl}/J$	Jackson Labs	Cat#012899; RRID:IMSR_JAX:012899
Mouse: NPY-gfp: B6.FVB-Tg(Npy-hrGFP)1Lowl/J	Jackson Labs	Cat#006417; RRID:IMSR_JAX:006417<
Mouse: Oprmfl/fl: B6; 129-$Oprm1^{tm1.1Cgrf}$/KffJ	Jackson Labs	Cat#030074; RRID:IMSR_JAX:030074<
Mouse: WT: C57BL/6		Cat#000664; RRID:IMSR_JAX:000664<